

# Modelling and Simulation of Onboard Wire Antennas for a 3U CubeSat

Umang Garg and Rutwik Narendra Jain

Department of Electrical & Electronics Engineering  
Birla Institute of Technology and Science, Pilani, India

**Abstract**— This paper discusses the results obtained and conclusions made from modelling and simulation of the on-board antennas for a 3U CubeSat being developed by Team Anant, a group of undergraduate students at BITS Pilani. The nanosatellite features a hyperspectral camera as its primary payload. The paper initially documents the reasons for selection of a turnstile antenna for downlink in the 435 MHz band of the UHF region, and a monopole for uplink in the 144 MHz band of the VHF region. Ansys High Frequency Structural Simulator (HFSS) has been used to carry out parametric simulations for desirable network matching, radiation pattern and directivity. Further, the effect of the metallic structure of the CubeSat is examined for optimization of antenna parameters. The rationale for arriving at two particular positions for the antennas on the CubeSat is elucidated based on electromagnetic compatibility (EMC). Two different positions for the antennas are arrived at and a comparative analysis is provided. Simulations and results are also presented on the mutual interaction of the two different antennas. It is important to design, model and simulate an antenna using electromagnetic CAD tools, especially for low cost CubeSat projects. The paper is an attempt to provide nano-satellite missions with a systematic strategy for modelling and analysing wire antennas.

## 1. INTRODUCTION

The Telemetry, Tracking, and Command (TT&C) system of a nanosatellite facilitates communication of data from the satellite to the Earth, and vice versa. Antennas are the agents that transmit this data by transducing binary signals into electromagnetic waves.

Our nanosatellite features a hyperspectral imaging payload, with the mission objective to take images which allow measurement of chlorophyll content of phytoplankton so as to estimate and monitor the quality of water bodies.

Hyperspectral imaging poses two challenges, a large image data cube size and high power consumption. Implementation of hyperspectral imagery on a CubeSat further aggravates the problem because of size constraints and limited power generation capabilities of small satellites. These and other practical considerations determine the selection of antennas and frequency bands for operation of the communication system, outlined in this section.

### 1.1. Frequency Selection

The International Telecommunications Union (ITU) coordinates and regulates the transmission of all radio communication. The ITU provides amateur HAM radio users certain frequency bands that are free to use and do not require a formal application to the ITU for their use. The CubeSat community commonly uses these amateur radio frequencies. Our nanosatellite's communication architecture is full-duplex, with the downlink in the 435–438 MHz range of Ultra High Frequency (UHF) band and uplink in the 144–146 MHz range of the Very High Frequency (VHF) band.

### 1.2. Antenna Selection

Figure 1 provides a representative picture of the types of antennas used by CubeSat launches worldwide [1].

The following points were kept in mind while deciding the on-board antenna types and configuration:

1. Since a beacon antenna has to be continuously working, it is not feasible to use a directional antenna for the beacon, as in that case continuous pointing has to be maintained and the power budgets on nano-satellites generally do not permit that.
2. The advantage of using a turnstile antenna is that it gives a circularly polarized signal and hence it is not required to orient the satellite, along its longer axis as there is no problem of polarization mismatch loss. This however comes at the cost of increased power requirement in comparison to a simple dipole.

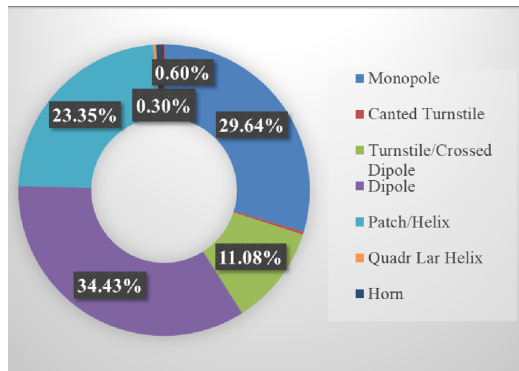


Figure 1. Pie distribution of types of antennas used by past CubeSat missions.

3. Approximately 70% of the CubeSats support Right Hand Circularly Polarized (RHCP) Ground Station [2].
4. Turnstile antenna usage also provides redundancy in the system, as one of the dipoles may also be used for reliable communication in an exigency mode.
5. A monopole is simple to construct. The radiation pattern for a monopole is not very directive, but if enough RF power is available from the ground station, then a monopole working in uplink is an effective choice.
6. Wire antennas are easy to integrate with a CubeSat because folding or looping of antennas is possible, thus achieving ease of compactness.

Based on these considerations, a crossed dipole or turnstile antenna was finalized as the downlink antenna, operating in the UHF band. The turnstile shall downlink both telemetry as well as housekeeping data to the earth station. The monopole antenna was finalized for up-linking data to the satellite from the ground station.

Table 1. Antenna configuration.

	Antenna Configuration	
	Antenna Type	Operating Frequency
<b>Uplink</b>	Monopole	144–146 MHz (VHF)
<b>Downlink</b>	Turnstile	435–438 MHz (UHF)

## 2. TURNSTILE

A crossed dipole turnstile antenna consists of two co-planar resonant dipoles placed at right angles to each other and fed with voltages of equal amplitudes and having a  $90^\circ$  progressive phase shift to produce circular polarization.

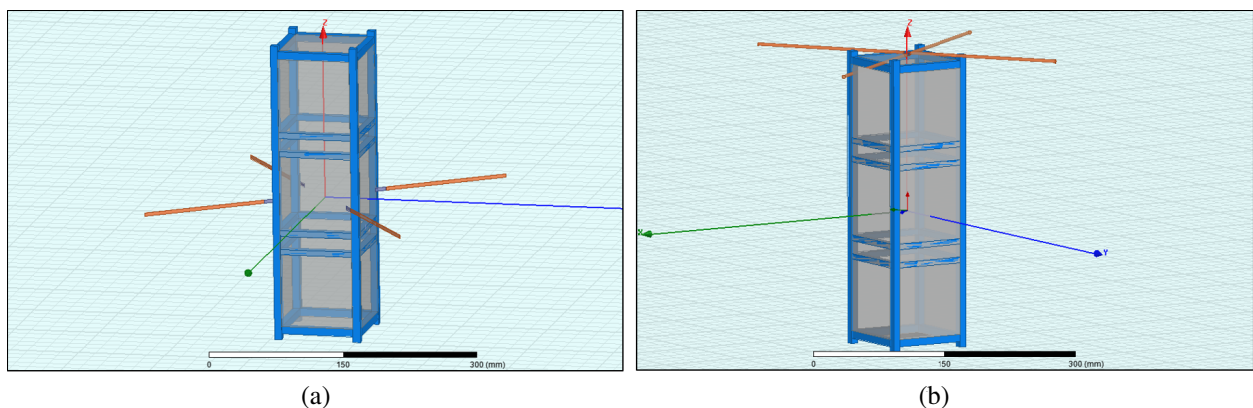


Figure 2. Turnstile antenna model with CubeSat structure (a) in position 1, and (b) in position 2.

The crossed dipole turnstile offers several advantages as an antenna for a Low Earth Orbit satellite [3, 4]:

- It can be used as a transmitting or a receiving antenna in UHF band to provide pure circular polarization, which is why it is not required to orient the satellite along its longer axis. In other words, there is no problem of polarization mismatch loss.
- We can switch between using two dipoles and/or a turnstile antenna, thus introducing redundancy in the system.
- Circular polarization gives better link margin and hence we can achieve higher data rate.
- The turnstile is simple and inexpensive to construct.

## 2.1. Modelling and Simulation

For practical low cost CubeSat applications, antennas are built out of measuring tape, typically made of stainless steel or beryllium-copper. This requires modelling of the antenna elements as rectangular or cuboidal strips.

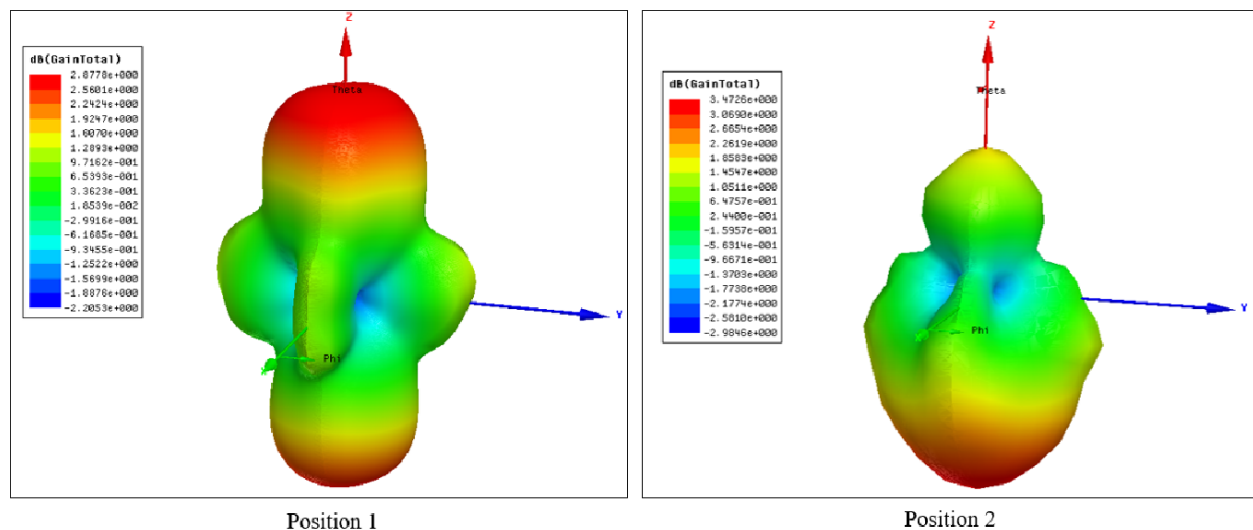


Figure 3. Radiation patterns produced by turnstile in positions 1 and 2.

According to the design considerations and limitations, two locations are finalized for the placement of our antennas. The position 1 as shown in Figure 2(a) includes the element of the turnstile to be fed centrally at a height of 156 mm from the base of the CubeSat. We follow a novel feeding scheme for the elements, thereby introducing multiple benefits in terms of radiation pattern and gain of the whole structure. Since the turnstile is a combination of two dipole antennas fed off-phase by  $90^\circ$ , with each of the dipole elements having a  $180^\circ$  phase shift in current between them, we employed a progressive phase scheme of  $0^\circ$ ,  $90^\circ$ ,  $180^\circ$ ,  $270^\circ$  fed to input voltage signal at the microstrip feed of different elements of this circular array. This implicitly emulates the functionality of the turnstile antenna. Also, the placement of each turnstile element is such as to increase the ground plane area availability, with each element getting an equivalent conductive ground width of 1.41 m in comparison to 1 m if the elements were placed in perpendicular to the face fashion. The initial length of each element and input impedance is chosen to be of a monopoles equivalent, i.e., 17.24 cm and  $36.8\Omega$  respectively, operating at 435 MHz. Fast sweep type in HFSS is preferred over Discrete solver in view of the solve time, and also over Interpolating sweep type due more accurate results over smaller simulation time frames. The Optimetrics approach of variation is subsequently used to produce refined results with respect to sweep input variables, i.e., element length, the feed gap and the width of the element. Due to the width constraints as well as the low sensitivity of the antenna parameters with respect to small change in width, the input variables in Optimetrics reduce to element length variation. The Optimetrics analysis result provides 14.7 cm as a suitable length to have a maximum impedance matching at the desired frequency of 435 MHz, shown in Figure 4(a).

A refined analytic solution is now developed for the optimized input variables. The analysis result as shown in Figure 6(a) yields an expected directional radiation pattern with RHCP gain of

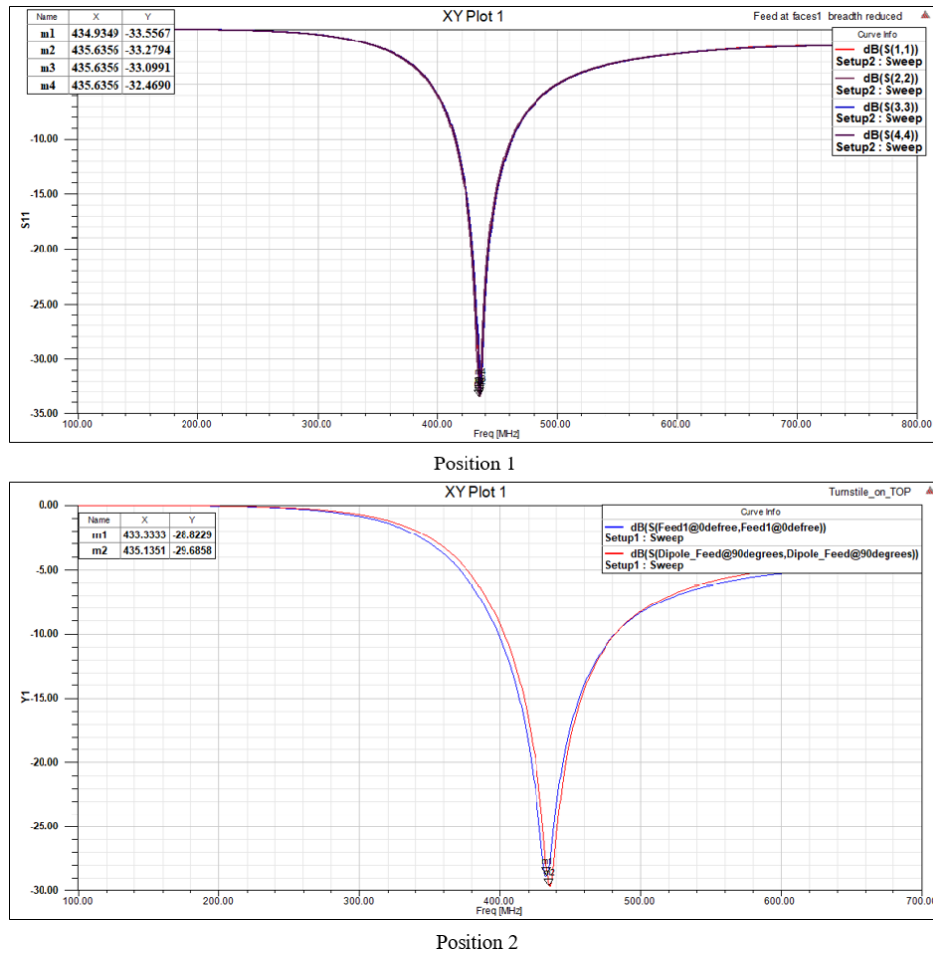


Figure 4. Reflection coefficient ( $|S_{11}|$ ) plots for turnstile in positions 1 and 2.

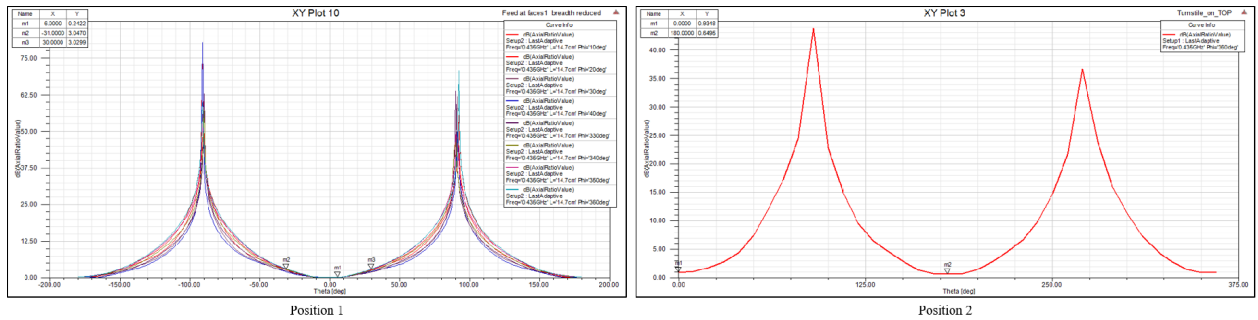


Figure 5. Axial ratio plots for turnstile in positions 1 and 2.

2.8 dBi and LHCP gain being  $-41$  dBi, thus showing uni-rotational nature of electric field vector of the EM wave in space. Axial ratio (AR) is important to verify the circular polarization of the radiated wave and our model has AR of 0.2 dB at the position of maximum gain as in Figure 5(a), much below the 3 dB standard. The perturbation in theta and phi about the maximum radiation zone is also suited to well-defined AR values. Thus, the results from simulation in Ansys HFSS provide proof of concept to model the turnstile as a circular array with each element having a symmetrical separation about the centre axis, fed progressively by a  $90^\circ$  phase difference in excitation.

Position 2 involves the turnstile on the top of the CubeSat face as shown in Figure 2(b). Here the dipoles are arranged in a crossed fashion, as shown in Figure 2, with a  $90^\circ$  difference of excitation source phases, where microstrip feeding is used. This basic turnstile faces the whole metal structure below it which channelizes the mirrored configuration and hence the radiation pattern is downward beamed. Figure 3 shows a comparative picture of the radiation patterns produced by the turnstile

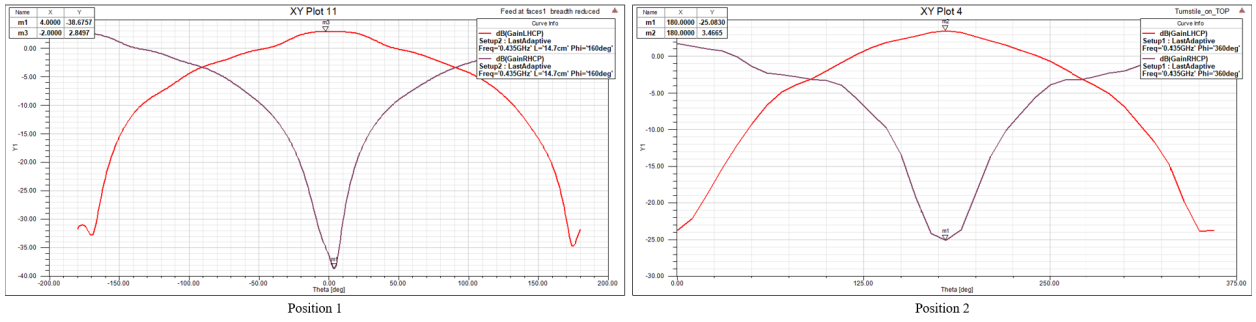


Figure 6. LHCP and RHCP Gain plots for turnstile in positions 1 and 2.

in positions 1 and 2. The two-dimensional cross-sections of these patterns in the phi and theta planes is presented in Figure 7. A microstrip feed line is used for the dipole elements with input impedance of  $73\Omega$  to match with the impedance of half-wave dipole. The optimetrics approach is applied after selecting the base length of the antenna to be 17 cm. The optimized solved length is computed to be 18.2 cm for maximum impedance matching and radiation as shown in Figure 4(b) at 435 MHz, our required solution frequency. The AR values for this configuration as shown in Figure 5(b) are 0.93 dBi, well within the boundary of 3 dB constraint. The impedance matching factor depicted by the S11 plot in Figure 4 shows  $-28$  dBi, perfect for fabrication.

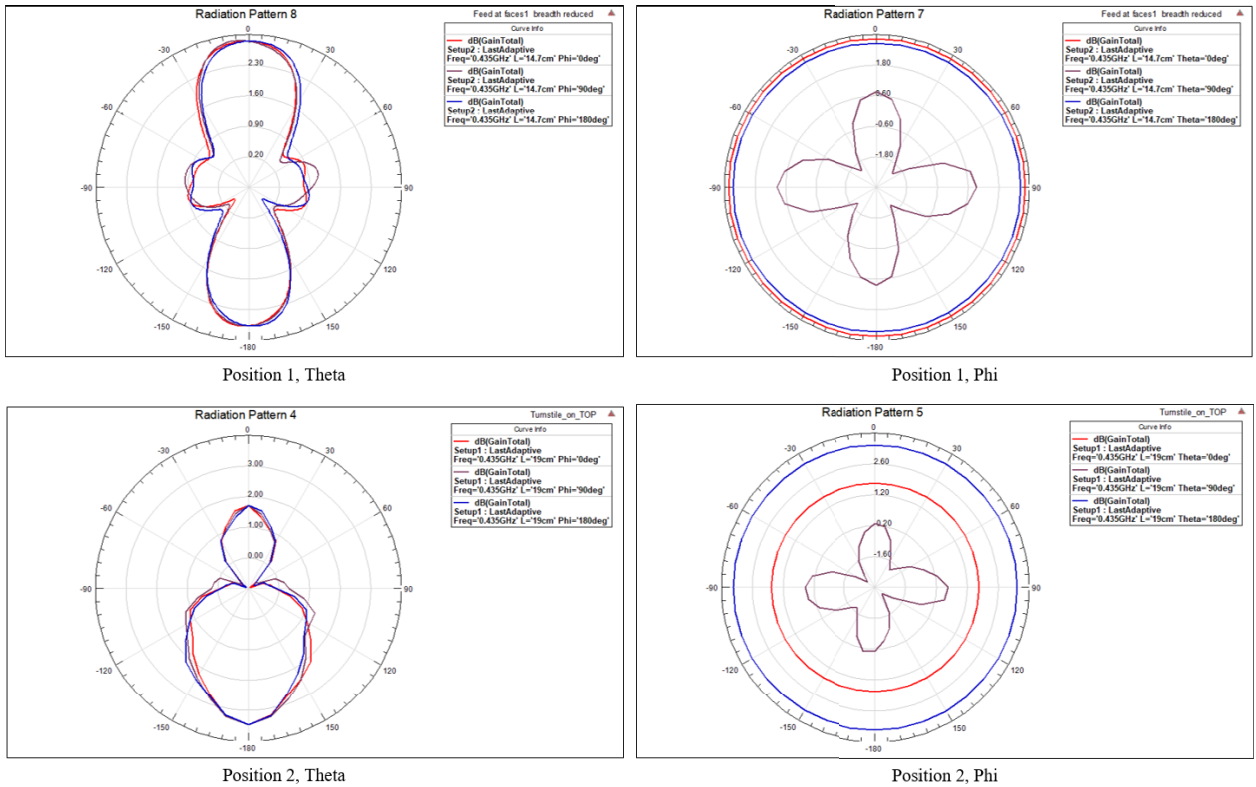


Figure 7. 2D radiation plots for turnstile in positions 1 and 2.

The common benefit of both locations deduced from the radiation pattern is that we do not need to employ  $180^\circ$  rotational actuation of the nanosatellite to focus the main lobe towards the earth, as it is automatically directed when the camera placed on the opposite face as of the turnstile is earth-pointed. Thus pointing for down-linking of data is equivalent to pointing for image capture.

### 3. MONOPOLE

As shown in Figure 1, about 30% of CubeSats use monopole antennas for communication. If communication requirements are omni-directional, such as that of a beacon antenna or an uplink

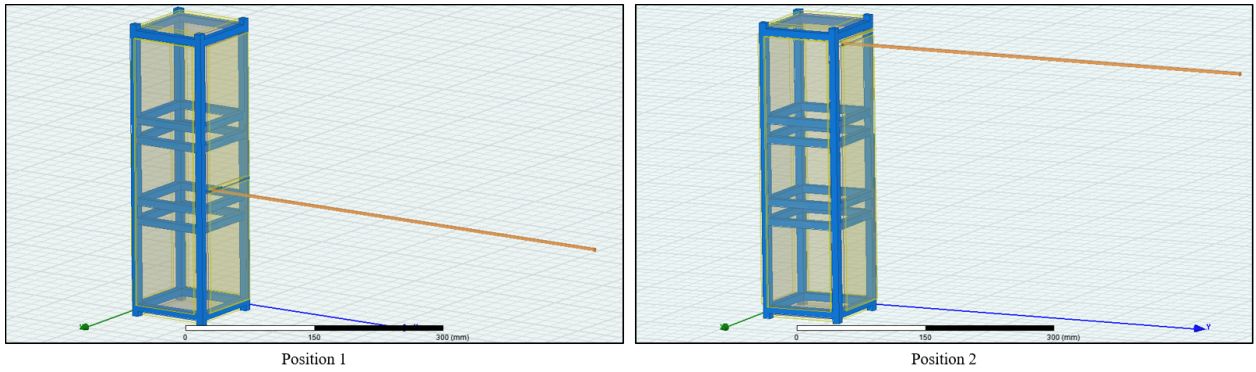


Figure 8. Modelling of monopole antenna in positions 1 and 2, relative to the CubeSat structure.

antenna, a monopole is well suited to the purpose. It offers additional savings because of less weight and length (typically quarter wave) compared to dipole. It is easier to be deployed as it does not require a balun for symmetric excitation as in the case of a dipole. A 144 MHz monopole is used for uplink of telecommand data from the ground segment.

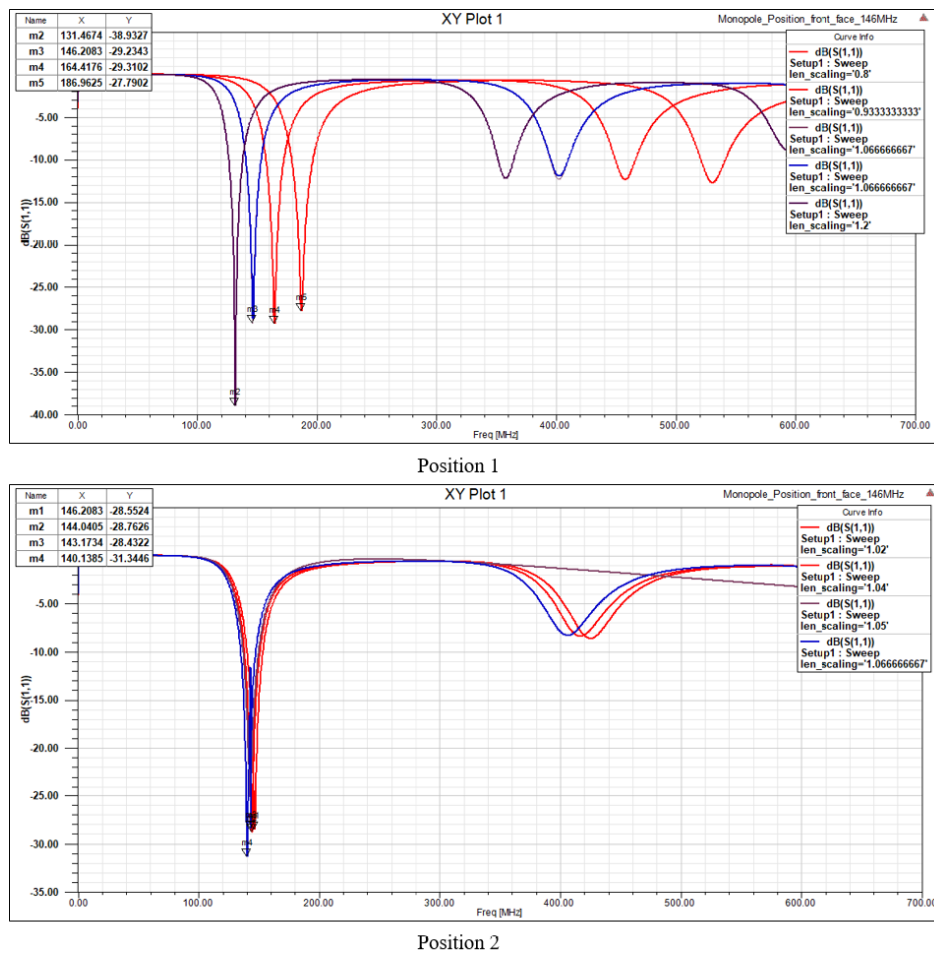


Figure 9. Reflection coefficient ( $|S_{11}|$ ) plots for monopole in positions 1 and 2.

### 3.1. Modelling

The basic model of the CubeSat frame was made according to the specifications provided by the mechanical and thermal subsystem. The frame is made up of aluminium rods and aluminium sheets on the faces. The monopole is then introduced in the structure using a cylindrical element whose length was initially taken to be  $(\lambda/4) = (2.05/4) = 0.5125$  m. This length is optimum for

small radius antennas as it provides good impedance matching. Though we are using the monopole antennas, we use the effective property of metals (here aluminium sheet) of charge induction to create an exact image of a radiating body, thus making the radiation pattern omnidirectional in nature, necessary for CubeSat missions. This virtually makes the monopole antenna operation to be as a dipole in free space with half the characteristic impedance  $Z_{in} = 36.5 + j21.25\Omega$  [5].

The feed to the antenna is provided by coaxial cable. To implement feeding we have used lumped port feed where the satellites panel serves as the ground plane. A small slot for the monopole is provided in the front face to complete the structure. The final model is shown in Figure 8.

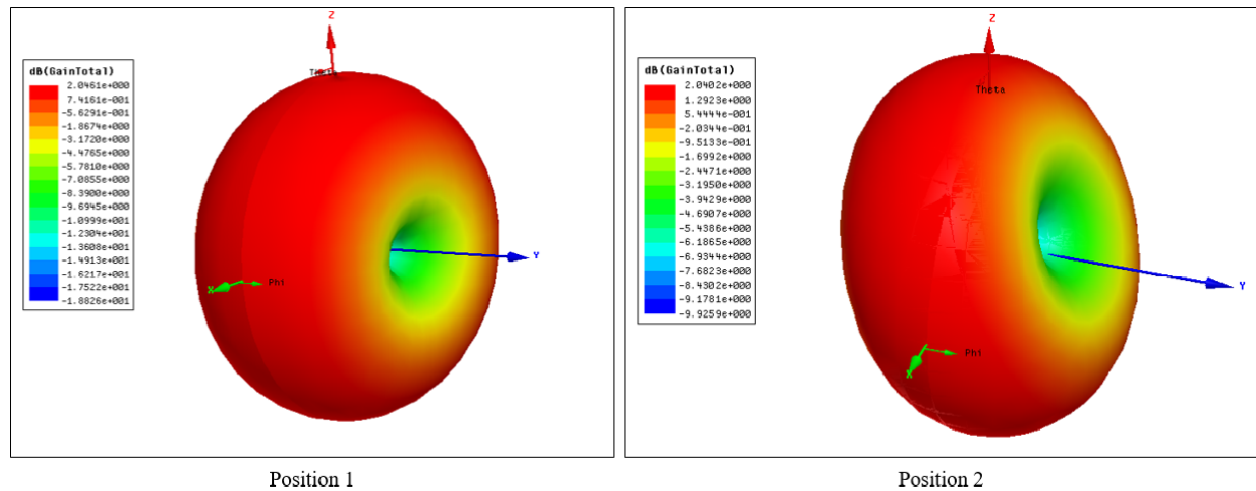


Figure 10. 3D radiation patterns for monopole in positions 1 and 2.

### 3.2. Results

The objective is to obtain maximum radiation gain and radiation efficiency at the desired frequency of operation of the monopole. The parameters which reflect this are S11 and Radiation Gain. Practical observation revealed that scaling of length is proportional to change in frequency at which maximum power transfer occurs. Also, larger width results in increased radiation gain by virtue of greater surface currents.

The motivation of the different available positions comes from similar constraints as for the turnstile antenna. ‘Fast’ sweep type is used for analysis. An Optimetrics analysis of parameters was set up including the length of monopole and its radius. Initially, a rough estimate of the best parameters was found out and a scaling factor of 1.067 for position 1 and factor of 1.02 for position 2 produced best results for the length scaling process. The radiation pattern and gain values as shown in Figure 10, are consistent with the predicted outputs with a significant improvement in monopole gain. The deviation from the literature maxima of 5.15 dB gain for monopole on a ground plane occurs due to practical limitations of the maximum conductive ground area availability.

## 4. MUTUAL COUPLING

The model of turnstile and monopole have been simulated separately and presented in the previous sections. However, it is imperative to observe the effects of electromagnetic interference between the two antennas for a complete picture. This section, therefore, details the mutual interference issues of these different EM components on the performance metrics of each antenna.

The reflection coefficient ( $|S_{11}|$ ) plot in Figure 9 shows that apart from its designed resonant frequency of 144 MHz, the simple monopole antenna also exhibits a resonant mode at around 420 MHz, close enough to the frequency of operation of the turnstile antenna. The radiation pattern at 435 MHz has a null at the centre as shown in Figure 11, which clearly shows that our antenna has second resonant frequency near 435 MHz and thus will hinder the normal operation of our turnstile antenna. On the other hand, the turnstile antenna has the first resonant frequency at 435 MHz itself and hence, negligible effect of the turnstile occurs on the monopole. In order to examine the possibility of the monopole and turnstile both resonating at the same UHF frequency, a coupled model was set up, as shown in Figure 12, with both antennas present.

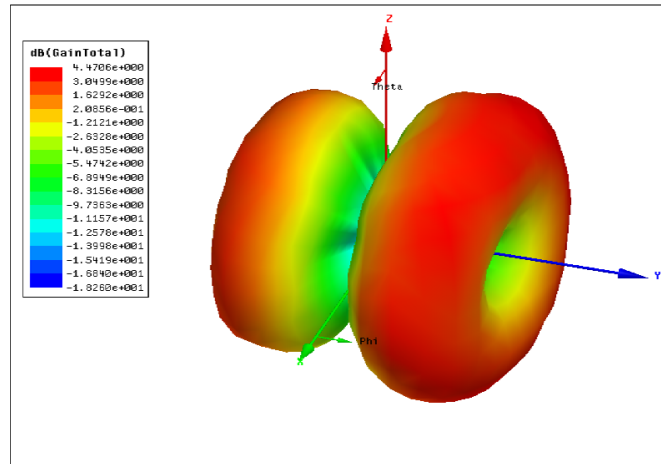


Figure 11. Radiation Pattern of monopole at 435 MHz, showing null at the centre.

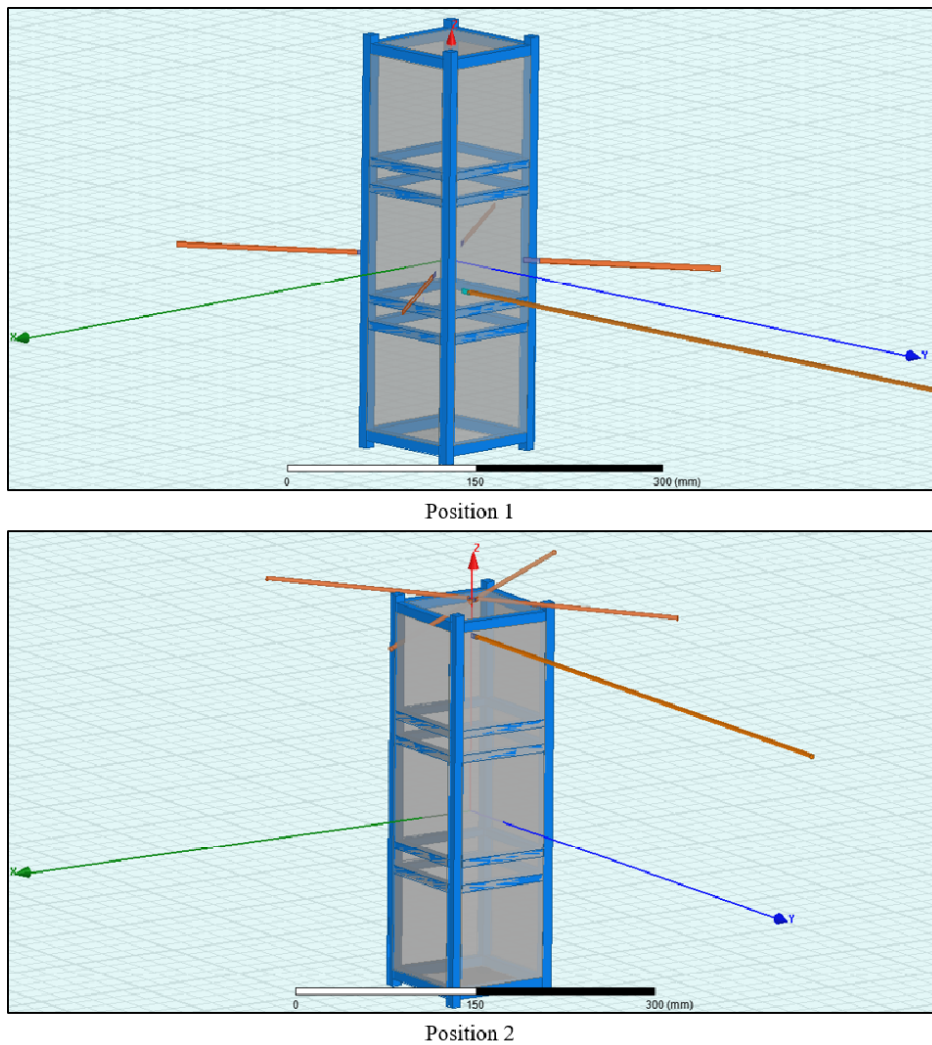


Figure 12. Positions 1 and 2 of the combined model, comprising of both monopole and turnstile.

The resultant radiation patterns are shown in Figure 13. The combined analysis yields that, as expected, only the turnstile radiation is affected by the monopole and not vice versa. Comparing the two positions, it is noted that the overall gain is slightly better in position 2. As compared to the standalone monopole simulation, the gain marginally deteriorates in position 1, while it marginally improves in position 2.

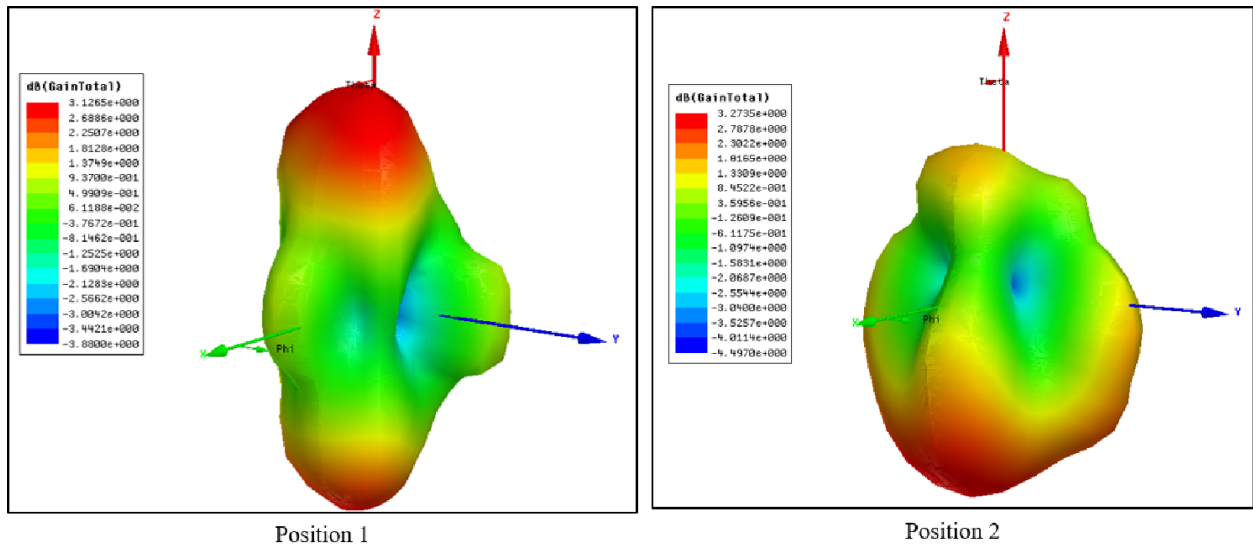


Figure 13. Radiation Pattern of combined model, for positions 1 and 2.

## 5. CONCLUSION

In this work, we have simulated wire antennas, namely monopole and turnstile antennas, for a 3U CubeSat. Lengths of the antennas are optimized using frequency scaling and parametric analysis. A novel technique for modelling phase-shifted sources for a turnstile is proposed, and relevant results are presented. LHCP gain is obtained under 3dB to verify circular polarization for the crossed dipole. Effect of structure and position of the antenna is examined through a comparative analysis of two positions. The effect of one antenna on another is also investigated using a combined analysis. Plots for the radiation pattern, reflection coefficient, two-dimensional gain in the theta and phi plane as well as axial ratios are presented in an ordered manner, so as to motivate a systematic strategy for modelling and analyzing antennas for CubeSats.

## ACKNOWLEDGMENT

The authors would like to thank Dr. Praveen Kumar A V, Assistant Professor, Department of Electrical and Electronics Engineering, BITS Pilani, for his technical expertise, support and guidance throughout the course of this work. The authors would also like to thank Dr. Kaushar Vaidya, faculty co-ordinator for Team Anant, the student nano-satellite project as a part of which this work was undertaken.

## REFERENCES

1. Klofas, B., *CubeSat Radios: From kilobits to Megabits*, SRI International, Ground System Architectures Workshop, Los Angeles, California, February 26, 2014.
2. Tresvig, J. L., *Design of a Prototype Communication System for the CubeSTAR Nano-satellite*, Department of Physics, University of Oslo, July 2010.
3. Darwish, S. G. M., K. F. A. Hussain, et al., *Circularly Polarized Crossed-Dipole Turnstile Antenna for Satellites*, 21st National Radio Science Conference, March 16–18, 2004.
4. Ta, S. X., I. Park, and R. W. Ziolkowski, *Crossed Dipole Antennas: A Review*, IEEE Antennas & Propagation Magazine, October 2015.
5. Awadalla, K. and T. Maclean, “Input impedance of a monopole antenna at the center of a finite ground plane,” *IEEE Transactions on Antennas and Propagation*, Vol. 26, No. 2, 244–248, March 1978, doi: 10.1109/TAP.1978.1141824.
6. Marholm, S., *Antenna Systems for NUTS*, TTT4530 Space Technology and Navigation, Specialization Project, Department of Electronics and Telecommunications (IET), NTNU, January 2012.